Algorithm Theoretical Basis Document for OSI SAF Medium Resolution Sea Ice Drift Product

OSI-407-a

Version: 2.3

Date: 19/09/2018

Gorm Dybkjaer

Document Change record

Document version	Software version	Date	Author	Change description
0.1		28.05.2009	GD	Submitted to review
1.0		08.07.2009	GD	Review for PCR
1.1		04.05.2011	GD	Edition for Preop.
1.2		16.02.2012	GD	Post ORR
2.0		28.02.2017	GD and Marcel König*	OCR w. uncertainties
2.1		28.02.2017	GD and Marcel König*	PCR approved
2.2		06.11.2017	GD	Corrections for ORR
2.2.1		02.03.2018	GD	ORR RIDs
2.3		19.09.2018	Eva Howe	Update to new template

*Marcel König, DMI intern from Kiel University, Germany

Table of contents

1. Introduction

This product of the Ocean and Sea Ice - Satellite Application Facility (OSI SAF) estimates sea ice displacement during a period between two satellite data swath that are separated by approximately 24 hours. The information available in the data set is geographical positions of sea ice, at the beginning and at the end of the 24h period. The data contains no information of the sea ice path between start and end of the drifting period.

The product is a gridded subset of the Northern Hemisphere (NH) covering the full OSI SAF-NH area (see figure 1). Due to the nature of the input data, each ice drift data set only contains valid ice drift data for parts of the output grid, and dummy values are filled in where no data are calculated.

The strength of this product lies in its relative high temporal and spatial resolution, in contrast to fully gridded data sets with longer ice drift periods and coarser spatial resolution. Moreover, a unique uncertainty algorithm has been developed and implemented for this product, providing individual uncertainties for each ice drift vector. The high spatial resolution, high precision and its uncertainty field makes this product suited for calibration and validation as well as for data assimilation in sea ice models.

The product is therefore aiming at modellers dealing with integrated sea-ice-atmosphere models and users dealing with merging of ice drift data sets, for both calibration and validation purposes.

1.1. Scope of this document

This Algorithm Theoretical Basis Document is describing the computational steps implemented for this Medium Resolution Sea Ice Drift processing software, which runs as part of the EUMETSAT OSI SAF programme. The document introduces and, to some extent, give justification for the scientific assumptions and choices made, that has led to present near-real-time sea ice motion processing in the EUMETSAT OSI SAF.

User related aspects of the product (like file format and output specifications) are to be found in the Product User's Manual [RD.2]. Results from validation against ground truth sea ice drift measurements will be gathered in an associated validation report which is in progress [RD.3].

General information on the EUMETSAT OSI SAF is available from the OSI SAF official web site (www.osi-saf.org).

After introducing some product specific notation in the remaining of current chapter, grid information, input data and processing steps are described in chapter 2. The algorithm behind the motion tracking algorithm is described chapter 3. The uncertainty algorithm is described in chapter 4 and the Validation strategy is explained in chapter 5. Finally, in chapter 6, the assumptions and limitations are discussed.

1.2. Common notations

A few product specific notations will be used throughout this document and to ease further reading the most central ones are explained here.

The main input data source for this ice drift detection procedure is thermal infrared data (***IR***) from the Advanced Very High Resolution Radiometer (AVHRR) on board Metop platforms. During the Arctic summer also visible data (***VIS***) from the same instrument is used as input data. The Arctic Summer is in this context defined as June, July, August and September.

The applied ice drift detection technique is based on feature recognition from one satellite swath data set to another. Here the data set recorded at time *T* is called the ***reference*** data, and the other data set used for feature comparison, recorded at time *T* + 24h, is called the ***compare*** data.

Two different data grids will be mentioned throughout this document. One grid is the ***input-grid***, which is a fixed 1 km grid in polar stereographic projection (table 1), containing either the *IR*- or the *VIS* data, i.e. brightness-temperature or albedo data.

The other grid is the product output grid, the ***ice drift-grid***, for which the ice drift data are calculated. The *ice drift-grid* is a 20 km resolution grid (table 2), in the same projection as the *input-grid*; i.e. an ice drift vector is produced for every 20 km, in case of cloud free conditions.

1.3. Glossary

Acronym	Description
AAPP	**A**TOVS and **A**VHRR **P**re-processing **P**ackage
AHA	A file format for gridded satellite data, designed at Swedish Met. and Hydro.Inst.
Argos	worldwide location and data collection system
ATBD	Algorithm Theoretical Basis Document (This document)
AVHRR	Advanced Very High Resolution Radiometer
CDOP	Continuous Development and Operations Phase
DAMAP	A common DMI/MET Norway software package for processing satellite data
DMI	Danish Meteorological Institute
EPS	EUMETSAT Polar System. The European comp. of a joint Europ./US polar satellite system.
EUMETCast	EUMETSAT's Broadcast System for Environmental Data
EUMETSAT	European Organisation for the Exploitation of Meteorological Satellites
GTS	Global Telecommunication System
ICEDRIFT-GRID	The fixed 20km grid in which the final ice drift product is delivered.
INPUT-GRID	The fixed 1km grid in polar steroid projection containing the input data, either the *IR*- or the *VIS*, from the AVHRR instrument.
IR	Infra Red
KAI	A EUMETSAT tool for processing EPS PFS format products
MCC	Maximum Cross Correlation
MET Norway	Norwegian Meteorological Institute
Metop	EUMETSAT OPerational METeorological polar orbiting satellite
NETCDF	A file format (network Common Data Form)
NH	Northern Hemisphere
NOAA	National Oceanic and Atmospheric Administration
NWP-SAF	The Numerical Weather Prediction SAF
OSI SAF	Ocean and Sea Ice Satellite Application Facilities
PROJ4	A cartographic projection library

PUM	Product User Manual
RMS	Root Mean Square
SAR	Synthetic aperture radar
SSM/I	Special Sensor Microwave/Imager
VIS	visible

1.4. Reference Documents

Reference number	Title	Acronym	Version	Release date
RD.1	Global Sea Ice Edge and Type Product User's Manual OSI-401-b OSI-403-b	PUM	1.3	May 2016
RD.2	Medium Resolution Sea Ice Drift Product User Manual OSI-407-a	PUM	2.0	Sep. 2018
RD.3	Validation and Monitoring Document for OSI SAF Medium Resolution Sea Ice Drift OSI-407-a	SVR	2.0	Sep. 2018
RD.4	Ocean and Sea Ice SAF CDOP-3 Product Requirement Document	PRD	1.1	Nov. 2017
RD.5	Evaluation of Medium Resolution Ice Drift Uncertainties - Input to MR-Icedrift (OSI-407) validation report. (Available in OSI SAF SVN)		2.1	Sep, 2017

1.5. EUMETSAT Disclaimer

2. Data and data handling

2.1. Input data

The input data used for this application is retrieved from the Advanced Very High Resolution Radiometer (AVHRR) instrument on board the polar orbiting Metop satellite. AVHRR instruments have been operating from polar orbiting satellites since the late 1970'ies on board NOAA satellites, and newer versions of the instruments carry 6 spectral bands, 3 in the visible spectrum and 3 in the near Infra-Red (IR) spectrum. Present application mainly operates with IR data, but during the Artic summer also a visible band is deployed. The bands applied as visible and IR data are channels 2 and 4, with central wave length of 0.86 and 10.8 microns, respectively.

The spatial resolution of the original input data is approximately 1.1 km at nadir, increasing towards the swath edges, and the scan width is 2045 pixels, providing a swath width of approximately 2800km. The accuracy of the geographical rectification is assumed to be sub pixel [EUMETSAT2007], with a maximum swath angle of ±56 degrees. This result in geographical accuracies between approximately less than 1 km at nadir and less than 2 km, at the edge of the swath (see chapter 6). The Metop satellite is sun synchronous, meaning that 2 swaths separated by 24h more or less cover the same area (figure 1 - right).

To avoid running the ice drift procedure for areas with no sea ice a sea ice mask is applied in the processing chain. The sea ice mask is the OSI SAF ice type product [RD.1] valid for the day of the *reference* data set.

The products availability timeliness, defined as the time from the last satellite input data arrival in the production centre to the product availability at the entry point of the distribution network, is 6 hours [RD.4]. This requirement is met by the OSI-407-a production.

2.2. Grid info

The two grids used in this procedure cover the geographical area OSI SAF NH [RD.1], illustrated in figure 1. The cartographic projection tool, PROJ.4 [PROJ4], is used to transform the grid positions in the NH subset into geographical coordinates and vice versa. Exact grid projection characteristics and grid size of the *input-grid* and *ice drift-grid* are given in tables 1 and 2, respectively.

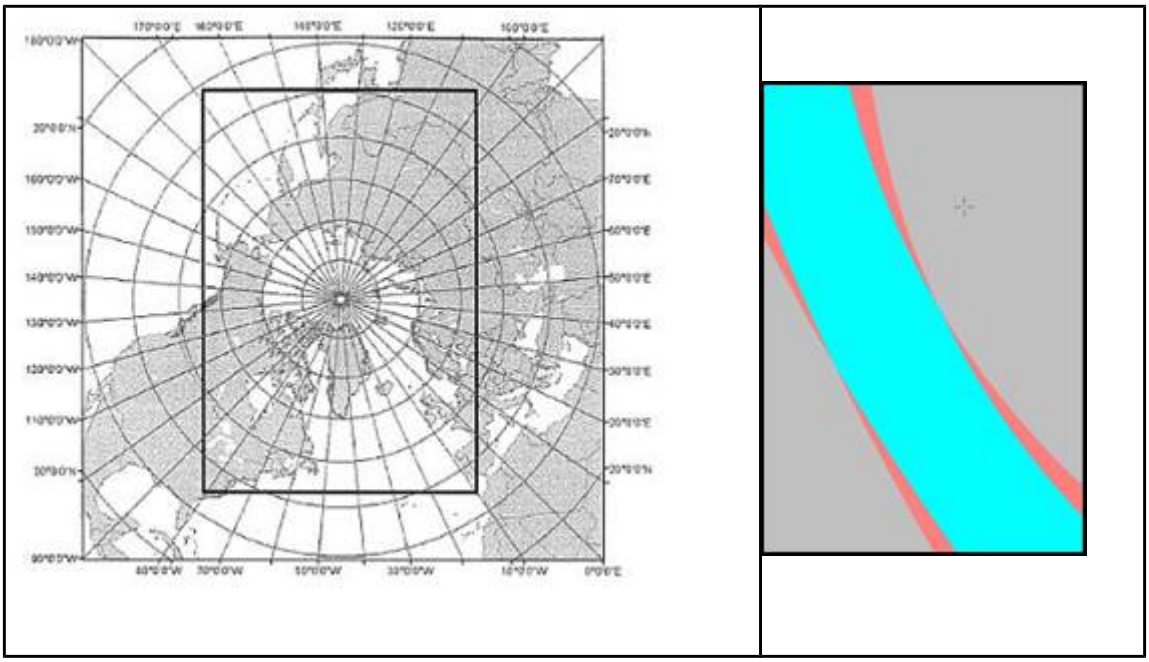

Figure 1 Left image: The OSI SAF NH-subset outlined with bold rectangle. Right image: The blue area illustrates the overlap between two input data sets separated by 24 hours for the NH area. Specifications of the grids are given in tables 1 and 2.

Table 1 Geographical definition of the *input-grid*.

Projection	Polar stereographic projection with true scale at 70^{o}N	
Resolution	1 km	
Size	7600	11200
Central Meridian	45^{o}W	
Corner points UL (dec.degr.)	32.655N	169.160E
Corner points UL (m)	U = -3800000	V = 5600000
Earth axis	a=6378273	b=6356889.44891
PROJ4-string	+proj=stere +a=6378273 +b=6356889.44891 +lat_0=90 +lat_ts=70 +lon_0=-45	

Table 2 Geographical definition of the *ice drift-grid*.

Projection	Polar stereographic projection with true scale at 70^{o}N	
Resolution	20 km	
Size	379	559
Central Meridian	45^{o}W	
Corner points UL (dec.degr.)	32.854N	169.114E
Corner points UL (m)	U = -3780000	V = 5580000
Earth axis	a=6378273	b=6356889.44891
PROJ4-string	+proj=stere +a=6378273 +b=6356889.44891 +lat_0=90 +lat_ts=70 +lon_0=-45	

In the product user manual [RD.2] the relations between grid coordinates and geographical coordinates are described.

3. Algorithm Description

Various setups of Maximum Cross Correlation (MCC) techniques are acknowledged and applied in many feature tracking programmes, not the least in programmes that keep track of drifting sea ice [Haarpaintner2006], [Maslanik1998], [Ezraty2006]. The technique is relatively straightforward to apply to gridded satellite data, and it is a relatively robust method. Moreover, the method is based on sensible assumptions for ice drift tracking (See chapter 6). There is no obviously better solution than the MCC technique for ice drift detection, hence the MCC technique is chosen for this application.

3.1. Algorithm principle

The applied MCC algorithm is a relatively simple pattern tracking technique that performs a section-wise matching of geographical distributed data recorded at time T (*reference* data, figure 2) with data recorded 24h later, at time T + 24h (*compare* data, figure 2). The best match, as measured by the highest correlation, between *reference* data and a sub-image/section of the *compare* data determines the ice drift for a given grid point.

For each point in the *input-grid* separated by 20 km, an ice drift vector is attempted retrieved by the iterative best matching routine sketched in figure 2, provided the ice drift-grid point is classified as sea ice according to the applied ice mask (see section 2.1). A matrix around each *ice drift-grid* point is correlated, to any corresponding matrix in the *reference* data that is inside the maximum allowed distance from origin in the *compare* data set, i.e. inside the red circle in figure 2, where the “maximum allowed distance…” is determined from a maximum allowed ice drift ‘speed’ multiplied with the time between the *reference* and the *compare* data sets. The shape of the cross correlation matrix (or landscape) between the *reference* and *compare* data sets is subsequently the basis for estimating the uncertainty of the final drift vector. I.e. the less ambiguous the maximum cross correlation value, the less uncertain is the ice drift vector (see chapter 4). The Maximum Cross Correlation landscape is defined by the correlation value for each grid point of the search box in the reference image in figure 2. That is one correlation value per 1 km grid step within the limits of a 51x51 matrix. The matrix size is defined by the maximum allowed drift speed of 25 km/24h inside approximately 24 h time lag between reference and compare data sets. Examples of MCC landscapes are shown in section 4.1.

The ice drift associated with a given *ice drift-grid* point from time T to T+24h is hence the geographical shift between the *ice drift-grid* point in the *compare* data set and the centre of the best matching matrix in the *reference* data set.

Despite the fact that the input data are highly sensitive to clouds, the production does not use any cloud screening procedures, instead a post MCC filtering routine is applied to remove erroneous data, i.e. ice drift vectors that are not coherent with its neighbourhood will be removed. (See section 3.2).

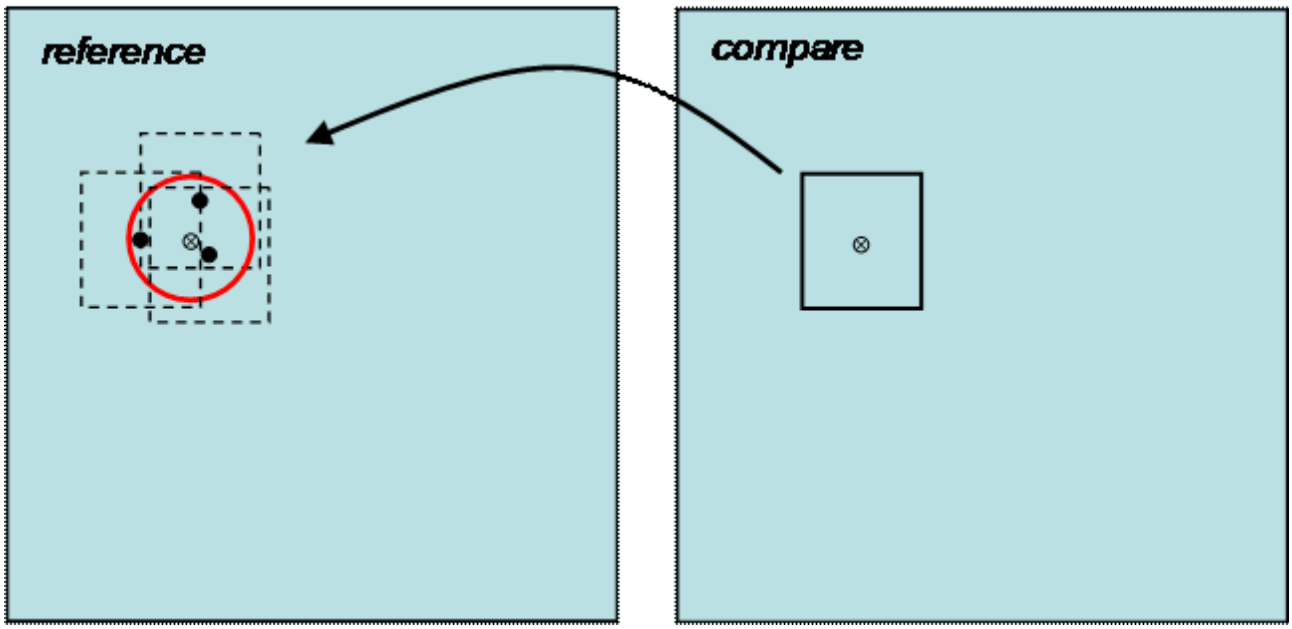

Figure 2 Sketch of the feature tracking procedure. Bold square in compare data illustrates the correlation matrix around the ice drift-grid point of interest (small circle with cross in reference and compare). Red circle in reference data correspond to the maximum allowed drift distance between the reference and compare data sets. The three punctured squares, with associate centers (black dots), illustrates 3 possible best matches (or maximum correlation matrices) to the compare matrix.

3.2. Filtering ice-drift vectors

Most ice drift estimation routines are associated with filtering routines to remove erroneous ice drift vectors. In this setup no cloud screening procedure is implemented, despite the fact that the input data are very sensitive to atmospheric properties. This consequently produce more erroneous ice drift vectors than routines based on micro wave data, that are much less sensitive to atmospheric opacity than IR and VIS data.

The reason for not applying cloud screening here is that cloud screening in the Arctic is rather dubious, due to comparable properties of cloud and snow/ice surfaces in the VIS and IR spectrum. Therefore, it is decided to ignore the presence of clouds and alternatively to run a comprehensive filter routine for erroneous ice drift vectors after the MCC routine. Whenever an effective cloud screening procedure is available for real time use, this will off course be implemented in the ice drift procedure. That will save time in the MCC procedure.

Obvious erroneous vectors are recognised by having an abnormal absolute drift compared to neighbouring ice drift vectors or a bearing that is uncorrelated to its neighbours. Figure 3 show an example of an ice drift product before and after applying the filter.

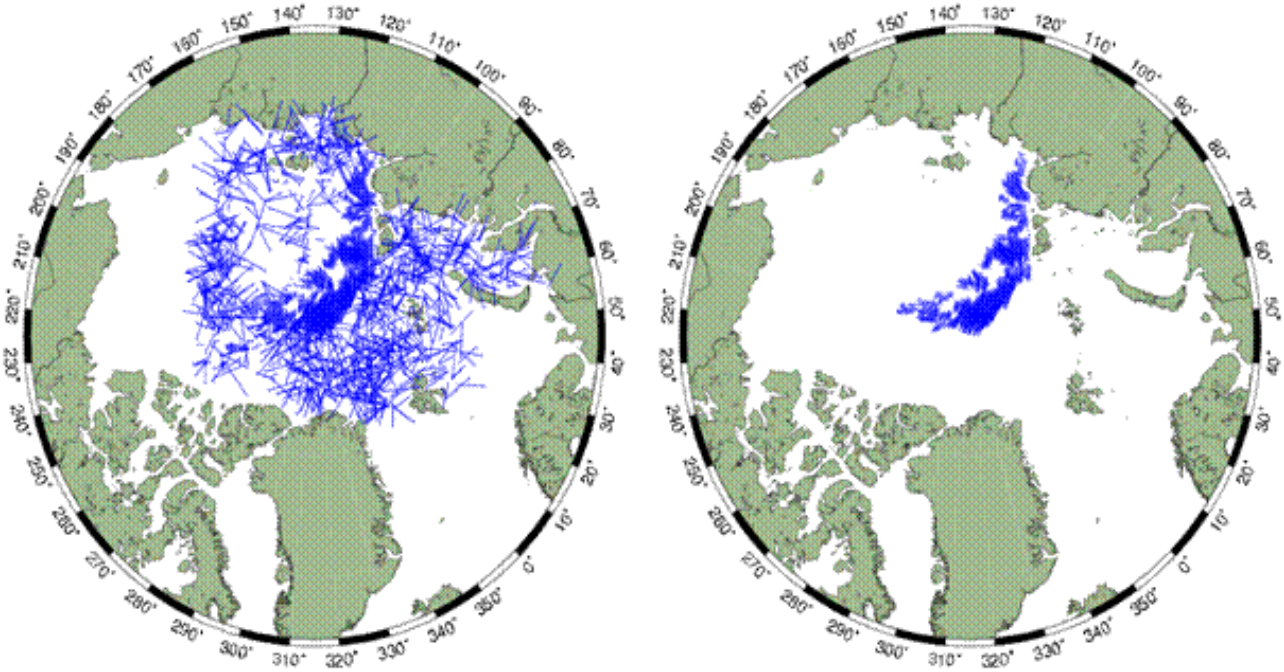

Figure 3 Example of ice drift estimation before applying filter (left) and after filtering of 'obvious' erroneous ice drift vectors (right). The lengths of the vectors are comparable, but scaled for presentation purposes.

1. Minimum Cross Correlation threshold
   - If the Maximum Cross Correlation between the *reference* and the *compare* matrices is less than 0.6, *this-vector* is dismissed.
2. Displacement length - neighbourhood homogeneity.
   - If the vector length difference between *this-vector* and the mean of all neighbouring pixels is larger than a given threshold, *this-vector* is dismissed.
3. Minimum number of neighbours.
   - If *this-vector* has less than 4 neighbouring drift vectors, *this-vector* is dismissed.
4. Direction - neighbourhood homogeneity
   - If the bearing of *this-vector* diverges more than a given threshold from the mean bearing of the neighbouring ice drift vectors - *this-vector* is dismissed.
5. Re-running filter number 3
   - After applying filter 1-4 to the non-filtered ice drift estimates, filter number 3 is re-applied on the remaining data, with minimum 4 neighbours.

The effect of the applied filter can be seen in figure 3, showing the un-filtered ice drift estimates and the final product. 'Neighbourhood' in filtering context is a 5 by 5 grid point matrix, around *this-vector*. So, 24 neighbours that are up to 2*20*√2 km away.

3.3. Algorithm characteristics

The characteristic numbers for this ice drift estimation setup are:

- The correlation matrix is 41*41 pixels in the *input-grid*, i.e. 41*41km
- The *ice drift-grid* is 20 by 20 km
- The maximum allowed ice drift speed over 24h is 0.3 m/s, i.e. fixing the maximum allowed 24h ice drifts to 25.92 km.
- ‘Neighbourhood’ is a 5x5 *ice drift-grid* matrix around the *ice drift-grid* point of interest.

4. Uncertainty algorithm

As mentioned in the “Algorithm description”, a spin-off of the MCC algorithms is a Maximum Cross Correlation surface, hereafter called the MCC landscape. The underlying hypothesis for the uncertainty algorithm developed here is that the MCC landscape, or cross correlation matrix, comprises information about the spatial uncertainty of each estimated ice drift vectors, namely, a well-defined maximum correlation peak has a smaller uncertainty than a `blurry' correlation surface with multiple correlation peaks or ridges. A sharp and narrow single peak in the MCC landscape indicates that a feature is unique in 2 dimensions, i.e. in both X and Y directions of the ice drift plane. Furthermore, features that are being tracked are relatively undistorted and easy to recognize in both the *reference* and in the corresponding *compare* data set. In this case we consider the ice drift estimate to be of good quality. Formal mathematical descriptions of the MCC landscape of each ice drift vector can thus be used to assess the error of individual drift vectors. The calculated error is subsequently transformed to uncertainty. The pilot study of this work is done by König (2016).

Six different MCC landscape categories are illustrated in figure 4, each representative for different sea ice scenarios or conditions: a) A single peak emerges from the MCC algorithm in case features are clearly recognized in both *reference* and *compare* data sets, and when the ice features are unique in 2D, i.e. in both X and Y displacement directions. This situation is assumed to provide the most certain ice drift estimate. b) Multi peaks can occur in case the spatial patterns repeat inside the area of interest. In this case, it is not clear which of the peaks represent the true drift, thus increasing uncertainty. c) A single ridge occurs when the MCC routine is tracking a straight sea ice lead and no other features are present. This gives a high cross correlation along the ridge, but no clear indication of the ‘true’ best match. d) Multiple parallel ridges provide uncertainties like the case of single ridge. e+f) Blurry MCC landscapes occur when the sea ice features are weak and/or are largely distorted from the *reference* to the *compare* data sets, e.g. in case of larger open water fractions, changing over the period of drift. This can cause large errors of the ice drift estimate and usually low maximum cross correlations. The aim of the uncertainty algorithm is thus to estimate the “peakedness” of the MCC landscape.

4.1. Uncertainty metrics

There exist no one metric to describe the peakedness of a complex landscape like a MCC landscape and this is in particular true for MCC landscapes that are not characterized by a well-defined peak. A large number of metrics have been tested in the development of this uncertainty algorithm, but many have been disqualified due to high inter-correlation with other metrics.

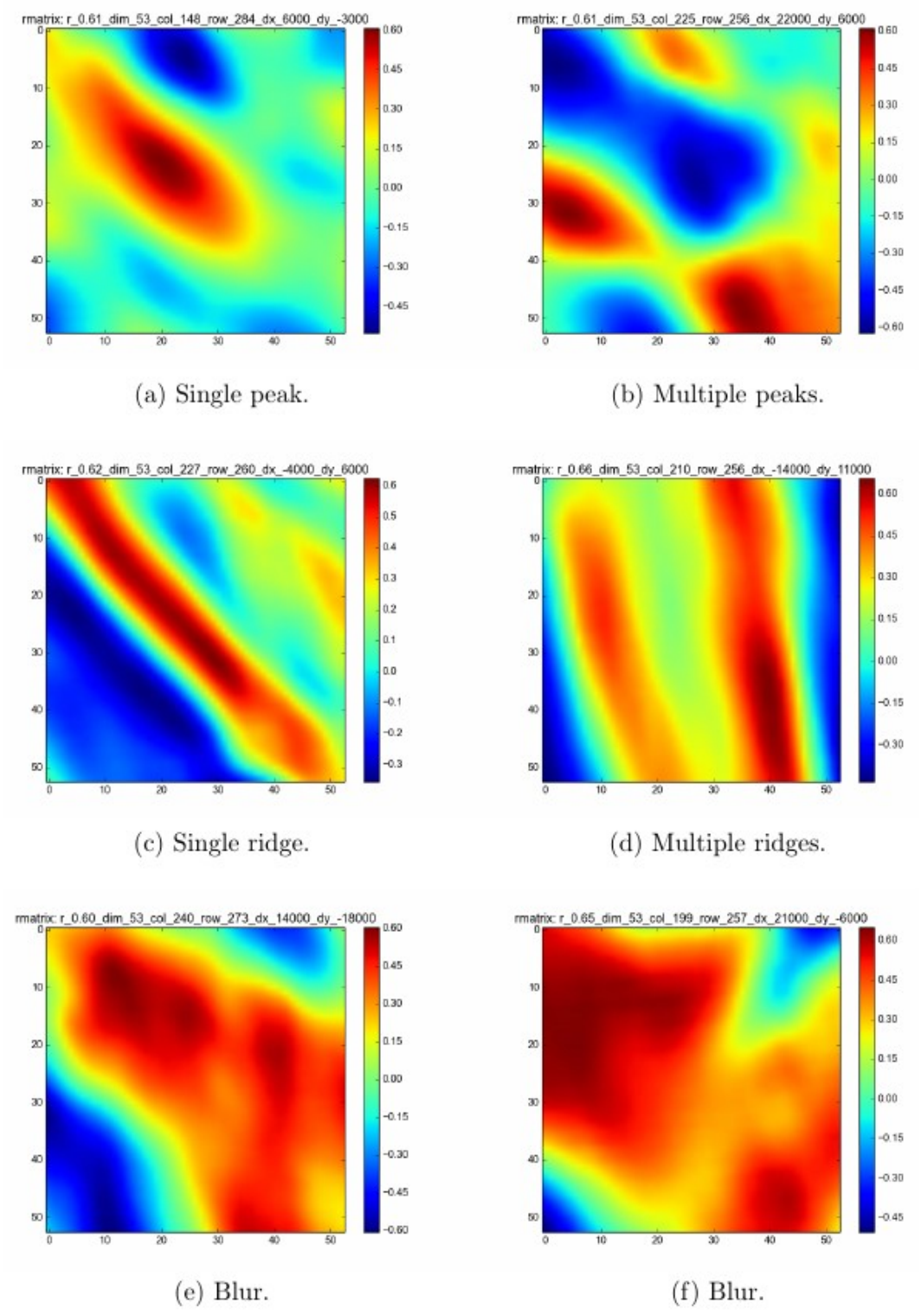

Figure 4 Maximum Cross Correlation landscape examples.

Here, seven metrics have been identified to contain unique information about the MCC landscape characteristics. Each of these metric are calculated for each ice drift vector estimate. Metric 1-4 are related to a 2D Gaussian fit to the MCC landscape and the remaining 3 are more or less independent

metrics. The applied metrics are adapted and inspired from Nickels and Hutchinson (2002), Xue et al. (2014) and Hollands et al. (2015).

Uncertainty matrices:

1. ***Sigma*** (Width of Gaussian fit, wide component)
2. ***Ratio*** (Ratio between the wide and the narrow sigma components, *sigmaw*/*sigman* of the Gaussian fit)
3. ***RMSE*** (Root Mean Square Error between the real MCC landscape and the Gaussian fit)
4. ***Gdist*** (Distance (in pixels, ~km) between peak of Gaussian fit and MCC landscape maximum)
5. ***Mdist*** (Mean distance of all pixels within 5% of the maximum correlation to the position of the maximum correlation pixel.)
6. ***PPR*** (The primary peak ratio, primary-peak/secondary-peak
7. ***PRMSR*** (Peak to root mean square ratio, see below)

Gaussian fit Metrics

Nickels and Hutchinson (2002) derive quantitative measures to describe the spatial uncertainty of feature trackers that are based on the sum-of-squared differences correlation method. In the scope of their work they fit a 2D Gaussian surface to a MCC landscape/surface. The same approach is adopted here. The standard deviations in the wide and in the narrow direction, *sigmaw* and *sigman*, respectively, can be used for the description of the actual MCC landscape. Small sigma values indicate a well-defined peak. Alternatively, a small *sigman* and a large *sigmaw* indicate a ridgy feature, as illustrated in figure 5. Large sigma values in both dimensions indicate more blurry features. Consequently, *sigmaw* and *sigman* values from a Gaussian fit contain valuable information about the uncertainty of an ice drift measurement. Here, sigmaw and the sigma ratio (the ratio *sigmaw*/*sigman*) are used as uncertainty metrics, ***Sigma*** and ***Ratio***, respectively. Furthermore, we use the Root Mean Square Error (***RMSE***) to describe the difference between the 2D Gaussian fit and the actual MCC landscape. The smaller the RMSE, the more well-defined single-peak, and therefore a more accurate ice drift estimate. The turning angle of the Gaussian fit is also computed and can be used to describe the direction of e.g. a ridge and thus a directional uncertainty. This is not utilized in this study. Further, Xue et al. (2014) argued that the location of the maximum of the Gaussian fit can be used to estimate sub-pixel displacement, based on the assumption “that the true displacement is within the primary peak region”. Here the displacement of the primary peak to the maximum of the Gaussian surface, the **Gdist** metric, is used as an indicator for ice drift vector uncertainty, because this value indicates how far from an ideal MCC peak the MCC landscape is. *Gdist* is the distance between the white and the red dots in figure 5.

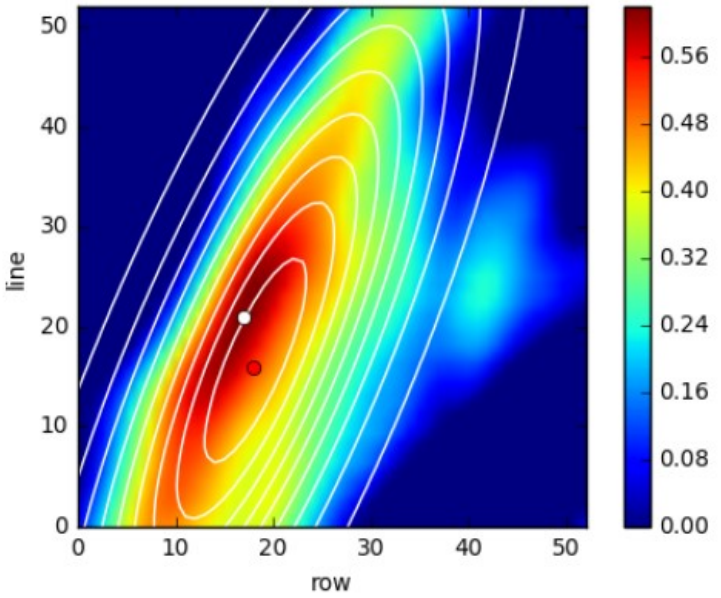

Figure 5 A 'ridgy' single peak MCC landscape and associated Gaussian fit (white contour lines). White dot is the point of maximum cross correlation (primary peak); red dot is maximum of the Gaussian fit. The distance between the two dots is defined as the Gdist metric.

MeanDistance Metric, Mdist

The MeanDistance, ***Mdist***, is a measure to evaluate how unique the maximum cross correlation values is. The Mdist is the mean distance of all pixels within 5% of the maximum correlation to the position of the maximum correlation pixel (see figure 6). In case of two or more similar high peaks (like figure 4b) the Mean Distance is high, and low for single peaks MCC landscapes, as shown in figure 6 right.

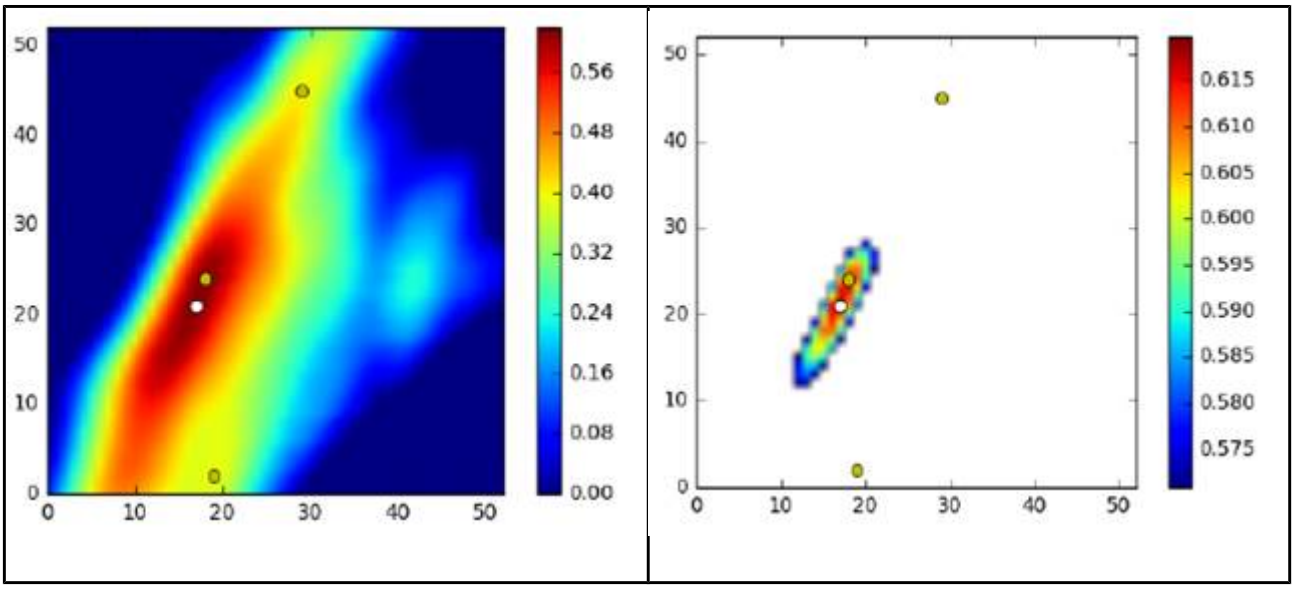

Figure 6 Left panel show a full MCC landscape, right is the area of the top 5% correlations. The MeanDistance metric, Mdist, is the average distance of all top 5% pixels to the maximum cross correlation value, indicated by the white dot.

PrimaryPeakRatio Metric, PPR

The primary peak ratio, ***PPR***, is the ratio between the height of the primary peak and the height of the second tallest peak, as illustrated in figure 7. This can also be considered as the signal to noise ratio. For PPR approaching 1, the uncertainty increases. However, we prefer a range between 0 and 1, we swap numerator and denominator (see uncertainty index, below).

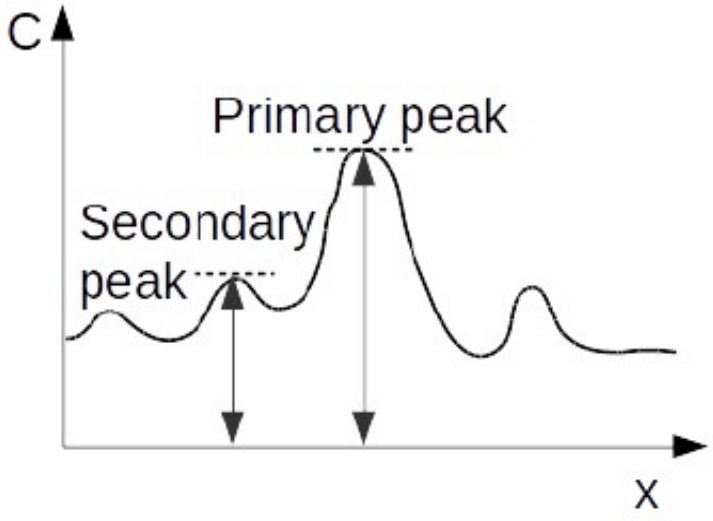

Figure 7 The Primary Peak Ratio is the ration between the primary peak and the secondary peak (from Xue et al., 2014).

Peak to Root Mean Square Ratio Metric, PRMSR

The peak to root mean square ratio, ***PRMSR***, is the "ratio between the magnitude of the cross correlation plane and square of the correlation plane root mean square value" (Xue et al. 2014), as illustrated in figure 8 and formalized in equation 1. This is similar to PPR, but is more focused on the signal to noise level, than PPR that focus on the 2 largest peaks and not on the baseline noise level.

Eq 1 PRMSR = $|Cmax|^{2/}$ $/Crms^2$, where

$$C_{rms}{}^2 = \left[\sqrt{\frac{1}{N_\Omega}\sum_{i\in\Omega}|C(i)|^2}\right]^2$$

From (Xue et al. 2014). This is illustrated in figure 8.

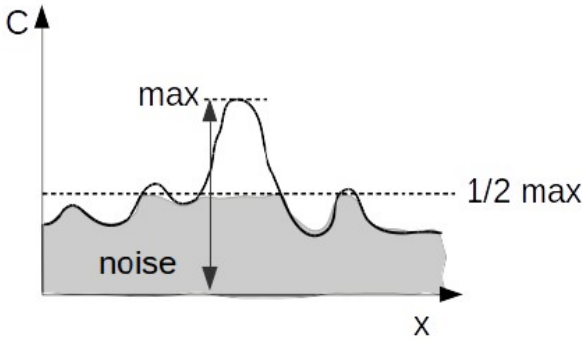

Figure 8 PRMSR is signal/noise: Where signal is Primary peak and noise is Gray area with C < max/2. (From Xue et al., 2014)

4.2. Ice Drift error Index

The estimation of ice drift uncertainties is done in two steps. First we determine a statistical ice drift error, E_{calc} (Eq. 2), and subsequently we scale E_{calc} to a corresponding observed uncertainty. Both steps are based on regression analysis.

The error estimate, E_{calc}, for each individual ice drift vectors is based on a regression analysis between the 7 uncertainty metrics and the corresponding observed error. E_{calc} is a mean error value that statistically will increase with increasing observed error.

E_{calc} is defined as the sum of the products of all uncertainty metric values and their weights, plus a constant values. Each metric weight is determined from a multivariate regression of approximately 6 month of collocated satellite ice drift data, and the corresponding observed drift from drifting buoys. The regression analysis uses the formulation in equation 2. The data sets used to train the error algorithm and validate the associated uncertainties are described in the validation report [RD.3].

Eq. 2 $\mathbf{E_{calc}} = k + a*\boldsymbol{Sigma} + b*\boldsymbol{Ratio} + c*\boldsymbol{RMSE} + d*\boldsymbol{Gdist} + e*\boldsymbol{Mdist} + f*\boldsymbol{PPR} + g*\boldsymbol{PRMSR}$

The coefficients of equation 2 were determined to be: k=75; a=-7.8; b=-4.8; c=3,149; d=2.2; e=1,937,796; f=553 and g=2.3. The impact from each uncertainty metric, on the calculated error is NOT reflected in the size of the coefficients them-selves, because each index have very different valid ranges, as illustrated in the validation report [RD.3].

4.3. Ice Drift uncertainty

From equation 2 we calculate a statistical error estimate for each ice drift vector. However, the nature of this error estimate is more an uncertainty estimate, than a precise error, because all components in the calculation are independent statistical indicators of errors. We therefore assume that the STD of observed ice drift errors is high among ice drift vectors with large E_{calc} and the STD is low among ice drift vectors with low E_{calc}-values.

If we plot the STD of observed errors as a function of E_{calc} we can justify whether the assumption of E_{calc} having the nature of uncertainty, is true. This is done in Figure 9, where the STD of observed ice

drift errors are binned into E_{calc} intervals of 300 m. The theoretical and ideal uncertainty line for observed uncertainty plotted against calculated uncertainty is also plotted in Figure 9. Now, by plotting the STD of observed errors as a function of E_{calc}, we use the theoretical 1:1 uncertainty limit (punctured black line) to assess whether E_{calc} is a good proxy for an uncertainty model. If the uncertainty model is good then the observed STD of errors should fit within and intersect with the 1:1 dashed lines for each E_{calc}bin. With a simple linear scaling this seems to be the case and we consider E_{calc} to be a proxy for ice drift uncertainty. We scale E_{calc} to the theoretical and ideal uncertainty, by applying a linear fit. This fit is illustrated by the blue dotted line in Figure 9. The fit is weighted by the number of samples in each bin. The fitted line is defined by: slope=1.08 and offset=269. The bin size of 300 m is selected as a compromise between having a sufficient number of samples in each bin and still to maintain a high resolution of the calculated uncertainty.

Minimum and Maximum uncertainties of 500 m and 2,500 m, respectively, are defined for the uncertainty algorithm. These limits are illustrated by the red dotted horizontal lines in Figure 9. The lower uncertainty limit is given by half the resolution of the input data and the upper uncertainty limit is ~2 times the STD of all errors in the test and training data sets, thus including ~95% of all data (see validation report [RD.3]).

The total calculated uncertainty (in meters) of any medium resolution ice drift vector, U_{total}, is now defined in equation 3:

Eq.3:

$U_{total} = 1.08 * E_{calc} + 269$; For $E_{calc} \geq 214$ and $E_{calc} \leq 2062$

$U_{total} = 500$ m ; For the E_{calc} less than 214 (= (500 m - offset)/slope)

$U_{total} = 2{,}500$ m; For $E_{calc} > 2062$ (= (2,500 m - offset)/slope) and IF one or more of the 7 uncertainty metrics cannot be calculated.

U_{total} is included in the ice drift product under the variable name *total_uncertainty*. See the Product User Manual, PUM [RD.1].

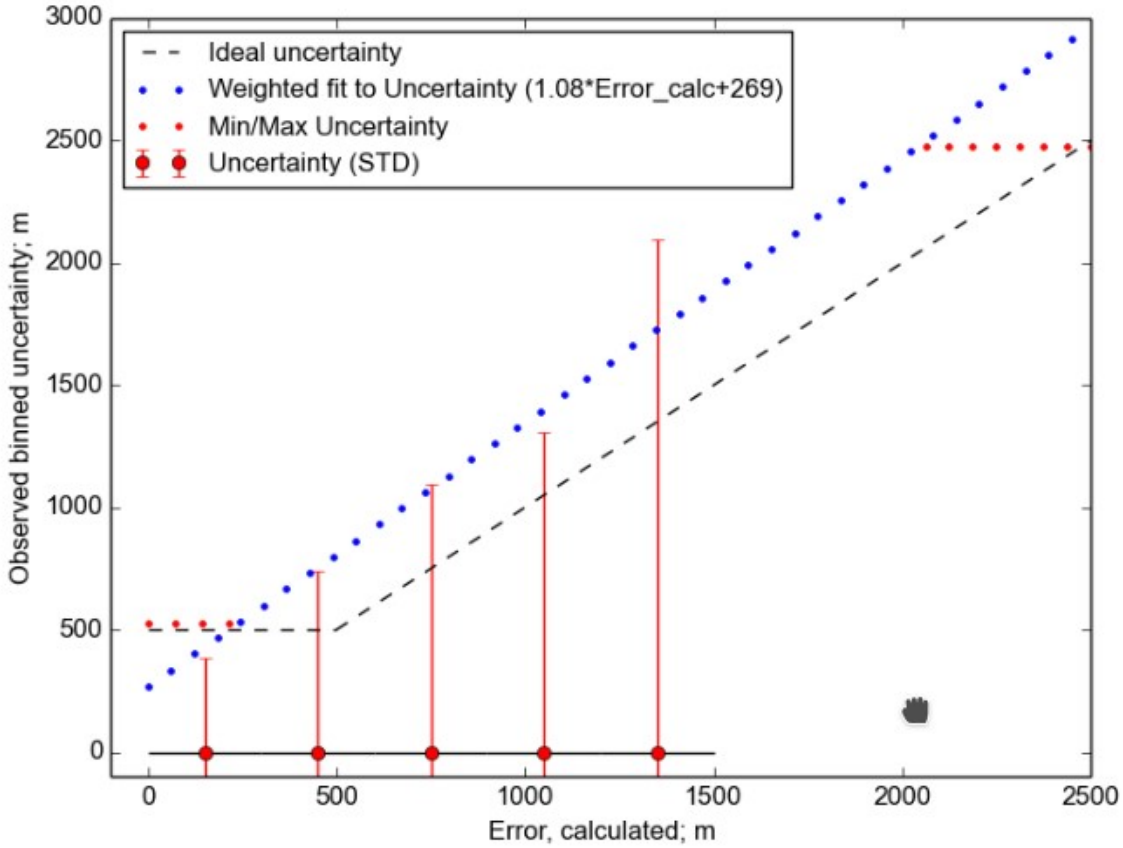

Figure 9Validation of uncertainties of the OSI-407 product. The x axis represent the calculated error, E_{calc}, and the y axis is the STD of the corresponding observed errors. The STD values are the standard deviations of observed errors (vertical solid red lines), within bins of 300 m of calculated errors. The blue dotted line is a weighted linear fit to all STD values with 10 or more samples, which transforms the E_{calc} to product uncertainty, U_{total}. (see text for explanation). The red dotted horizontal lines represent the minimum and maximum uncertainty limits. Black punctured line is the theoretical and ideal uncertainty limit for observed uncertainty plotted against theoretical uncertainty.

5. Validation strategy

A product specific validation report is prepared [RD.3] and also an ice drift product comparison report is finalized through a visiting scientist program [Hwang and Lavergne, 2010]. In these documents comprehensive validation work is carried out. The validation report contains statistics for approximately one year of ice drift data. It contains RMS errors, absolute error and correlation statistics, shown in table 3. Here are correlations between the satellite ice drift and buoy drift for two directional components, U and V. Also the RMS error, mean absolute error and bias are calculated.

Beside the general validation report, monthly validation is worked out with statistics comparable to the general validation report. This monthly report will be based on ‘on the fly’ validation statistics generated for each ice drift data set. The uncertainty estimates will be validated to the extent that validation data are available in sufficient numbers.

Table 3 Validation example for the ice drift product based on all available Argos buoy data in the GTS network. Valid for January 2009 (see also figure 10).

Directional validation	
Correlation delta U	0.937015
Correlation delta V	0.903716
Number of samples	1483
Absolut displacement validation	
RMS Error	1.37 km
MEAN absolut Error	0.91 km
Bias (buoy-sat)	-0.03 km

In figure 10 the data the validation values in table 3 are plotted as a scatter plot.

All validation is based on buoy data retrieved from the GTS network at DMI. Each buoy data is paired to all ice drift estimates within a vicinity of 50 km. Though it is well known that the Argos positioning system can be associated with errors, these data are never the less a comprehensive data set available in near real time, which is needed for ‘on the fly’ validation.

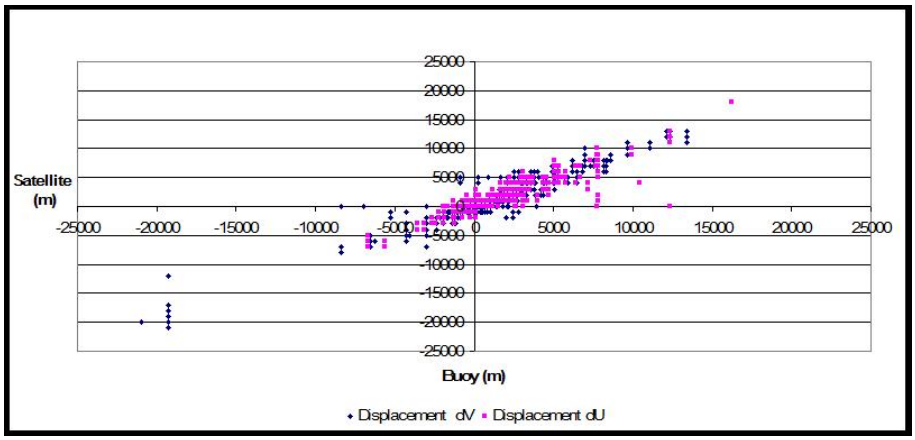

Figure 10 A scatter plot showing buoy drift and satellite estimated ice drift for U- and V-directions, where the U and V directions are oriented right-left and up-down, respectively, in the NH subset in figure 1 and specified in tables 1 and 2. The data are the basis for the error statistics in table 3.

6. Limitations and assumptions

No single data source exists that can fulfil all needs for ice drift data sets. Large scale and low resolution data, from passive microwave instruments like SSMI and AMSR(-E), can provide full Arctic coverage on a daily basis. However, the spatial resolution is coarse and using such data ice drift estimation for less than 48h only makes limited sense (see Lavergne2009). Such data are suited as input for large scale modelling, general sea ice circulation studies and climate studies.

On the other hand, SAR sensors can provide very high resolution ice drift information unaffected by atmospheric properties, but these data have only limited spatial coverage, resulting in only partial Arctic coverage on daily basis.

In between these high and low resolution microwave data sources are the AVHRR VIS and IR data. They provide very wide swath data, at medium spatial resolution and high repetition rate, suitable for 24h ice drift estimation. Short ice drift period and high spatial accuracy and resolution make the data suited for calibration and validation purposes and to some extent also for data assimilation. The uncertainty algorithm of this product is unique and may eventually be used for low and high resolution ice drift datasets.

6.1. Limitations

Due to the sensitivity of VIS and IR data to atmospheric water, the AVHRR data cannot provide fully gridded ice drift data on a daily basis. For a given area of interest both *reference* and *compare* data must have clear sky conditions in order to calculate ice drift. This limits the use of AVHRR data for surface analysis.

During the arctic summer this limitation is pronounced, as clouds often cover large parts of the arctic region. In periods with surface melting (summer), the contrasts in the IR data are drastically reduced and consequently making surface feature analysis difficult. During that period, this ice drift procedure uses VIS data, as this naturally coincide with periods with midnight sun. Despite the substitution of IR data with VIS data in the summer period, the data frequency drops to about 12 % of data frequency around January, where the cloud cover is at a minimum. Ice drift data frequencies for both IR and VIS data are plotted in figure 11, for a 9 month period.

6.2. Assumptions

The basic principle behind this feature tracking routine is the assumption of conservation in the features being tracked, i.e. the shape of the features must appear relative similar in both *reference* and *compare* data. This must comply to a degree where the correlation between the *compare* image correlates to the *reference* image with a correlation value, r, greater than 0.6.

It is also assumed that features of interest have no or limited rotation only.

It is further assumed that the net 24h displacement does not exceed 0.3 m/s and finally the feature being tracked must have 2-dimentional characteristics. I.e. if the feature is a straight lead exceeding the correlation matrix, the MCC routine will calculate a ‘ridge’ of almost equally high correlated match ups between the two images and hence make the best match between *reference* and *compare* data dubious. This will be captured by more of the uncertainty indices, as described in chapter 4, and use of the uncertainty indices is thus recommended. In summary the assumptions can be expressed like this:

a) No or little change in feature shape between *reference* and *compare* data.

b) No or little rotation.

c) Maximum 24h drift of ~25km.

d) 2-dimentional feature inside the image matrix, use of uncertainty indices is recommended

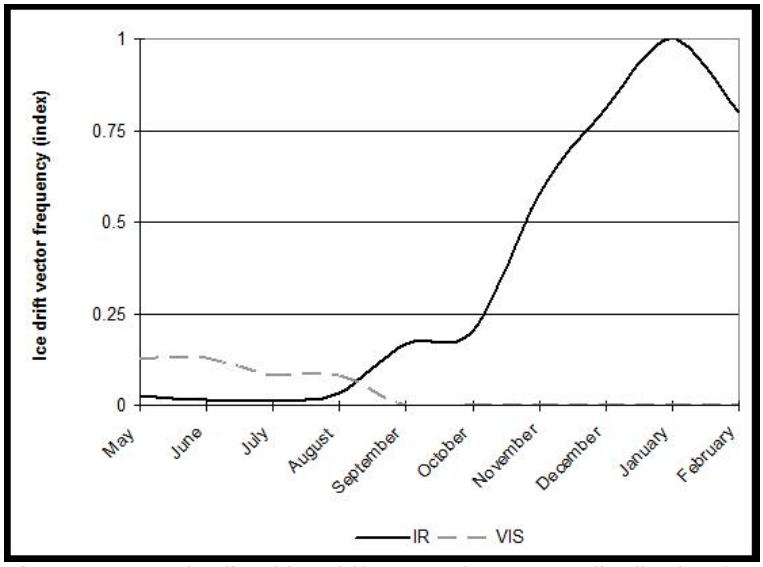

Figure 11 Standardized ice drift vector frequency distribution for IR and VIS data, for an area North of Greenland, during 9 month of 2005-2006. During summer the successful retrieved ice drift vectors from IR data are practically zero in comparison to the number of ice drift vectors during winter. During spring and summer the successfully retrieved ice drift vectors from VIS data are approximately 12 percent of the maximum ice drift vector frequency in January and February.

7. Reference

EUMETSAT. 2007. EPS Operations Services Specification, January 17th.

Ezraty, R., F. Arduin and Jean-Francios Piollé. 2006. Sea Ice Drift in the central Arctic estimated from Seawinds/Quickscat backscatter maps. IFREMER, Users Manual version 2.2.

Haarpaintner, J. 2006. Arctic-wide operational sea ice drift from enhanced-resolutionQuikScat/Sea-Winds scatterometry ands its validation, IEEE Trans. Geoscie. Remote Sens.,vol. 44, no.1, pp.102-107.

Hollands T., S.Linow and W.Dierking. 2015 Reliability Measures for Sea Ice Motion Retrieval From Synthetic Aperture Radar Images. IEEE Journal of Selected Topics in Applied Earth Observations and Remote Sensing. 8 (1), pp. 67-75 .

Hwang, P. and T. Lavergne, 2010. Validation and Comparison of OSI SAF Low and Medium Resolution and IFREMER/Cersat Sea Ice drift products. Reference: CDOP-SG06-VS02. http://osisaf.met.no/docs/OSISAF_IntercomparisonIceDriftProducts_V1p2.pdf

König, Marcel. 2016 An uncertainty estimation for sea ice drift vectors. Internship report, DMI and University of Kiel.

Laverne, Thomas. 2009. Algorithm Theoretical Basis Document for the OSI SAF Low Resolution Sea Ice Drift Product. SAF/OSI/CDOP/met.no/SCI/MA/130.

Maslanik, J., M. Drinkwater, W. Emery, C. Fowler, R. Kwok and A. Liu. 1998. Summary of ice-motion mapping using passive microwave data. National Snow and Ice Data Center (NSIDC) Special Publication 8.

Nickels K., S. Hutchinson, 2002 Estimating uncertainty in SSD-based feature tracking, Image and Vision Computing 20, pp 47-58.

PROJ4. http://trac.osgeo.org/proj/

Xue, J. J, Z.. Charonko, P. P. Vlachos, 2014 Particle image velocimetry correlation signal-to-noise ratio metrics and measurement uncertainty quantification, Measurement Science and Technology 25, 11.